A SENSOR FAULT-TOLERANT CONTROL SOLUTION BASED ON CURRENT OBSERVERS APPLIED TO THREE PHASE INDUCTION MOTOR DRIVE

Cuong Dinh TRAN[1,*], *Giang Thi Tuyet LAI*[2], *Thao Minh CA*[2], *Thong Tien NGUYEN*[2], *Phuong Duy NGUYEN*[3]

[1] Power System Optimization Research Group, Faculty of Electrical and Electronics Engineering, Ton Duc Thang University, Ho Chi Minh City, Vietnam.
[2] Faculty of Electrical and Electronics Engineering, Ton Duc Thang University, Ho Chi Minh City, Vietnam.
[3] Faculty of Electronics and Telecommunication, Saigon University, Vietnam.

*Corresponding Author: Cuong Dinh Tran (Email: trandinhcuong@tdtu.edu.vn)
(Received: 18-May-2023; accepted: 07-Agust-2023; published: 30-Sep-2023)
http://dx.doi.org/10.55579/jaec.202373.413

Abstract. *This paper presents a fault-tolerant control (FTC) solution to enhance the reliability and sustainability of a three-phase induction motor drive (IMD) against open circuit sensor failures (or total sensor faults). The motor speed control in the investigated drive will operate based on a field-oriented control (FOC) strategy. A typical FTC function consists of two main processes: fault detection of feedback signals from the sensors and reconfiguration of the control methods. This paper proposes using two-phase current observers to diagnose various sensor failures, and then the corresponding sensorless methods are applied to the control reconfiguration. Using MATLAB/SIMULINK software, the IMD-integrated FTC function was operated and tested under different fault conditions. Simulation results have proved that the IMD-integrated FTC function has worked stably and sustainably even in sensor failure conditions.*

Keywords

rotor field-oriented control, fault-tolerant control, sensorless control, total sensor fault.

1. Introduction

The induction motor is an electrical device widely produced globally, used in many fields, such as high-power exhaust fans, oil-extracting mills, the mining and textile industry, but most notably in the electric car manufacturing industry, replacing traditional gasoline-powered engines [1].

In the recent period, the IMD system has made significant progress by utilizing powerful algorithms to overtake limitations of nonlinear structure in electromagnetic relationships, making IMD a popular choice for applications that require high precision control, replacing DC drives [2]. A typical IMD system consists of four main components: motors, a power inverter, a controller unit, and a measurement system (sensors).

The effectiveness of controlling IMD relies on stable constructions of the motors, an accurate analytical model, and high-quality signals from sensor systems. All components in the system must possess sufficient capacity and stability to ensure optimal performance [3].

Various fault diagnosis methods have been developed for IMDs, each targeting specific types of errors. This study focuses on sensor failures in harsh environments of IMD operation, such as exposure to liquids or solid contaminants, impact effect, electric shock, mechanical vibration, etc. These problems can lead to sensor failure or disconnection of the feedback signal, resulting in the entire system failing to function. Detecting and resolving sensor faults is crucial to enhancing the sustainability of IMDs. Therefore, implementing sensor FTC strategies integrated into IMD controllers to mitigate sensor failures has been the subject of extensive research in advanced control in electrical machines [4].

At present, FTC techniques are divided into two main categories: the first is the active fault tolerant control branch (AFTC), and the second is the passive fault tolerant control branch (PFTC) [5]. The PFTC approach aims to ensure system stability during predefined failures without requiring fault diagnosis and reconfiguration processes. PFTC's benefits are its independence from fault detection and offline operation. Nevertheless, PFTC only targets a few defined simple malfunctions. The performance of PFTC depends on additional hardware structures, which will raise the expenses of the drive [6].

On the other hand, IMDs integrated AFTC utilize measured signals from the sensor to identify the real-time operational status of the motor and apply the proper control techniques without additional hardware. The standard AFTC functions in the closed control loops include three procedures: sensor fault diagnosis, wrong signals isolation, and reconfiguration control mode. In general, AFTC systems have the capability to solve multiple types of faults without additional hardware; nevertheless, the performance of AFTC functions mainly relies on fault detection time and unmistakable accuracy among sensor error types to enhance the operational stability of the IMD system. The following section reviews and examines the fault diagnosis techniques that belong to the AFTC class.

The FOC is a modern method for the speed controlling of IMDs. The IMs using the FOC method can accurately control both the torque and the flux by applying the orthogonal components of the current vector corresponding to a rotation coordinate line in the rotor flux [7–10]. An IMD that uses precise control algorithms such as FOC will require accurate feedback from sensors, typically consisting of at least two current sensors integrated into the converter and one mounted speed sensor at the rotor shaft for obtaining efficient operation. The accuracy of these feedback signals is essential for the stability and reliability of the motor control algorithm. Hence, if these signals' errors are not handled correctly, the system can be damaged or destroyed, causing great harm. As a result, integrating FTC functionality will enhance the reliability of the IMD against sensor faults.

Based on the FOC technique, a measured speed signal from a sensor is essential for controlling the required torque to achieve the desired speed in IMDs. Therefore, if the measured speed signal is defective, a proper signal must be used to replace it immediately. The paper [11] uses the extended Kalman filter (EKF) as a velocity estimator for generating virtual speed operating in parallel with the measured signal during the regular operation of the drive. The difference in comparison between the virtual speed signal and the measured speed with a predefined threshold value to identify a speed sensor fault conditions. Likewise, the paper [12] utilizes a current-based MRAS observer to calculate the speed of the rotor; Based on that, the fault condition of the encoder will be determined based on the increase in the difference between the measured signal and the estimated signal. [13] has employed the mean deviation of twenty data points of the measured speed and the reference speed to detect the fault condition occurring with speed sensor. The authors in [14] suggested an approach to determine a speed sensor failure by employing a stator flux observer, thereby improving the operation of the IMD across the entire range of velocities. The paper [15] recommended the usage of two-speed observers, namely EKF and Luenberger Observer (LO), in conjunction with a speed sensor. EKF's calculated signs are incorporated into the fault detection algorithm for low and medium-speed zones. At the same time, the other observer is utilized to detect faults in the speed encoder corresponding to the high-speed ranges. An alternative technique outlined

in [16] introduced the diagnostic method that detects malfunction of the speed encoder by analyzing the variation between measured currents and virtual currents.

The current signal configuration for IMDs can be categorized into two forms based on the structure of the drive: integrating three current sensors and integrating two sensors. According to the IMD system employing three sensors for feedback currents, the diagnostic strategy based on Kirchhoff's law corresponds to the principle that the sum of currents in a three-phase system is always zero under normal conditions. Three observers constructed based on each of the corresponding two-phase currents are used to determine the fault of the current sensors. This means that when a fault occurs with a particular phase of the stator current, the two observers, according to that particular phase current, will be affected; otherwise, the other observer will still function normally without being affected. Therefore, the wrong phase can be diagnosed due to the according fault conditions [17, 18]. The article [19] utilized the Luenberger Observer to estimate a current space vector for diagnosing current sensor faults. The feedback current and virtual currents were subsequently compared to their according phases for each pair in the $[a, b, c]$ coordinate to determine the wrong phases.

Nonetheless, when the IMD is equipped with two current sensors, employing Kirchhoff's law principle to detect current sensor malfunctions becomes impractical. The authors in [20] proposed a straightforward and efficient technique for diagnosing fault currents that compare the virtual current's magnitude to the magnitude of each measured phase current. Nevertheless, a main limitation of this method is the fault confirmation duration of roughly one cycle, which renders it unsuitable for deployment in the low-speed range (owing to its extended fault detection duration). In [21], a fault detection technique using an asymmetry index computed as the deviation between the RMS values of the two-phase currents is proposed to determine current sensor fails. To diagnose current sensor failures, an axis transformation methodology based on the Park formula has been suggested [22]. Similarly, another technique employing a space vector comparison algorithm combined with a delay function in priority order [23] was used for rapidly detecting current sensor failures at low-speed zones. The third-difference operator was applied in [24, 25] to diagnose measured current signal failures. The strength of this method is its sensitivity to unusual changes in the measured signal. Nevertheless, this algorithm may confuse with the random noise, resulting in misdiagnosis.

This paper proposes a diagnosis method based on two current observers to detect both speed sensor and current sensor failure corresponding to open circuit faults (or total sensor faults). After determining the fault type, the false signal will be isolated, and the related sensorless technique will be applied to control the motor speed.

2. Sensor fault-tolerant control based on current observers

The proposed sensor FTC solution applied to the three-phase IMD is presented in this part.

2.1. The machine model of the three-phase IM based on the FOC technique

The relationship between electrical parameters in induction motors is nonlinear. In the stationary coordinate $[\alpha, \beta]$, the machine equations are described as follows:

$$\mathbf{u}_S^{St} = R_S \mathbf{i}_S^{St} + d\boldsymbol{\Psi}_S^{St}/dt \tag{1}$$

$$\mathbf{0} = R_R \mathbf{i}_R^{St} + d\boldsymbol{\Psi}_R^{St}/dt - j\omega_r \boldsymbol{\Psi}_R^{St} \tag{2}$$

$$\boldsymbol{\Psi}_S^{St} = L_S \mathbf{i}_S^{St} + L_m \mathbf{i}_R^{St} \tag{3}$$

$$\boldsymbol{\Psi}_R^{St} = L_R \mathbf{i}_R^{St} + L_m \mathbf{i}_S^{St} \tag{4}$$

where

$\mathbf{u}_S^{St}$: voltage in vector form;
$\mathbf{i}_S^{St}/\mathbf{i}_R^{St}$: stator/rotor current in vector form;
$\boldsymbol{\Psi}_S^{St}/\boldsymbol{\Psi}_R^{St}$: stator/rotor flux in vector form;
R_S/R_R : resistance of stator/rotor;
$L_S/L_R/L_m$: inductance of stator/rotor/magnetizing.

The FOC method is utilized to speed control based on independent control of rotor flux and

torque by separating the current space vector into two perpendicular components $[x, y]$. The i_{Sx} controls the rotor flux as the rated value, and the i_{Sy} controls torque [9]. Figure 1 shows the separation of the stator current space vector in detail.

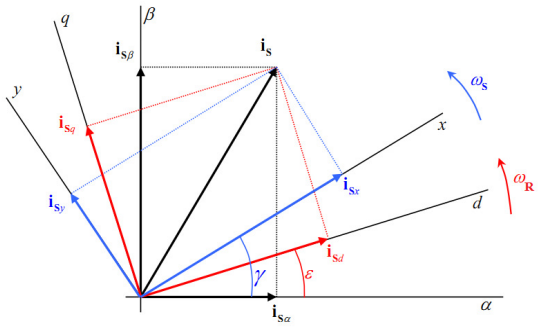

Fig. 1: Vector diagram of FOC method.

The real-time stator currents $[i_a, i_b, i_c]$ are transformed into the stationary coordinate $[\alpha, \beta]$ by applying Clarke formulas as follows:

$$\begin{bmatrix} i_{S\alpha} \\ i_{S\beta} \end{bmatrix} = \frac{2}{3} \begin{bmatrix} 1 & -0.5 & -0.5 \\ 0 & \sqrt{3}/2 & -\sqrt{3}/2 \end{bmatrix} \times \begin{bmatrix} i_a \\ i_b \\ i_c \end{bmatrix} \tag{5}$$

Corresponding to the FOC control technique, the current components in $[\alpha, \beta]$ coordinate are converted to the rotating coordinate $[x, y]$ according to Park formulas:

$$\begin{bmatrix} i_{Sx} \\ i_{Sy} \end{bmatrix} = \begin{bmatrix} \cos(\gamma) & \sin(\gamma) \\ -\sin(\gamma) & \cos(\gamma) \end{bmatrix} \times \begin{bmatrix} i_{S\alpha} \\ i_{S\beta} \end{bmatrix} \tag{6}$$

where: γ is the rotor flux angle [9].

The formulas (7) and (8) present the relationship between rotor flux-torque with stator components in the $[x, y]$ coordinate system.

$$i_{Sy} = \frac{1}{p} \frac{2}{3} \frac{L_R T_e}{L_m \psi_R} \tag{7}$$

$$\psi_R = \frac{L_m}{1 + T_R} i_{Sx} \tag{8}$$

Therefore, the motor torque and speed will be controlled independently, corresponding to the current components in the FOC method.

2.2. Sensor fault-tolerant control

The speed control system of the IMD will be integrated with the FTC function to determine the status of the feedback signals from the sensors and select the appropriate control method. This integrated actuator structure is illustrated in Figure 2.

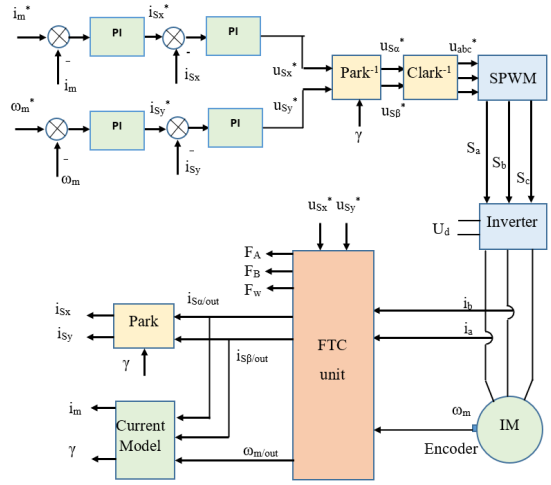

Fig. 2: The control structure based on FTC-FOC.

During operation, the state of stator currents and motor speed will be feedback to the controller through sensors. Corresponding to the control structure that integrates the FTC function, the measured signals will be analyzed and evaluated for health status by the FTC unit before being provided to the FOC loop. If the feedback signal from a sensor is appropriate, the output of the FTC will be the corresponding measured signals; otherwise, if the feedback signal is faulty, the FTC will reject the false signal and provide the corresponding estimated signals.

Figure 3 depicts the basic structure of the FTC in feedback signal processing. Speed sensorless methods such as MRAS. Sliding mode will be applied to calculate the estimated speed from the measured currents and reference voltages [26]. Correspondingly, appropriate current sensorless methods will be used to generate virtual currents [27]. In this paper, the estimated rotor speed will be calculated by RF_MRAS refer to [28, 29], and the virtual current will be de-

termined by Luenberger observer-based current estimator [30].

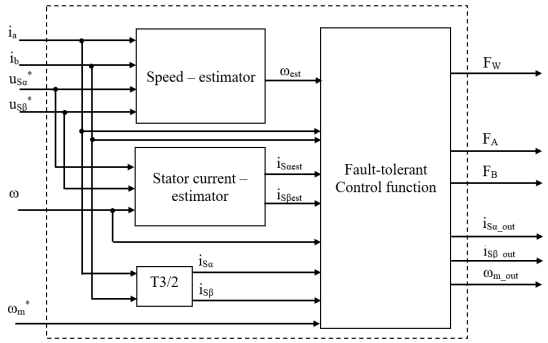

Fig. 3: The FTC function.

Two components of the virtual stator current in $[\alpha, \beta]$ will be transferred into $[a, b, c]$ coordinate systems by the reverse-Clarke's formulas as follows:

$$\begin{bmatrix} i_{aest} \\ i_{best} \\ i_{cest} \end{bmatrix} = \sqrt{\frac{2}{3}} \begin{bmatrix} 1 & 0 & 1/\sqrt{2} \\ -0.5 & \sqrt{3}/2 & 1/\sqrt{2} \\ -0.5 & -\sqrt{3}/2 & 1/\sqrt{2} \end{bmatrix} \times \begin{bmatrix} i_{S\alpha est} \\ i_{S\beta est} \\ 0 \end{bmatrix} \tag{9}$$

Two observers using a comparison algorithm between estimated current signals and the measured currents will be applied to determine the status of the measured signals of the sensors.

$$\begin{aligned} &Ob_a : If(|i_a - i_{aest}| > Th_i)\,\{Ob_a = 1\}; \\ &Ob_b : If(|i_b - i_{best}| > Th_i)\,\{Ob_b = 1\}; \end{aligned} \tag{10}$$

where: Th_i is the limitation of the deviation between measured and virtual currents. Based on checking simulation results and referring to some research journals, a 10% rated current value can be set as a limitation of these comparison formulas [22, 23].

Based on the two observers' results, each sensor's feedback state will be determined as in Table 1, the corresponding fault flags of each sensor will be shown as shown in Table 2, and the FTC will provide the appropriate output signal, as shown in Table 3.

3. Simulation results

In the Matlab/Simulink environment, a three-phase IM model is simulated based on an actual

Tab. 1: Sensor state.

Sensor state	Ob_a	Ob_b
Healthy	0	0
A-phase current Fault	1	0
B-phase current Fault	0	1
Speed Fault	1	1

Tab. 2: Sensor Fault Flag.

Sensor state	F_A	F_B	F_W
Healthy	0	0	0
A-phase current Fault	1	0	0
B-phase current Fault	0	1	0
Speed Fault	0	0	1

Tab. 3: Outputs of FDI unit.

Sensor state	Outputs: $i_{S\alpha\ out}$, $i_{S\beta\ out}$, $\omega_{m\ out}$
Healthy	$i_{S\alpha}$, $i_{S\beta}$, ω_m
A-phase current fault	$i_{S\alpha est}$, $i_{S\beta est}$, ω_m
B-phase current Fault	$i_{S\alpha est}$, $i_{S\beta est}$, ω_m
Speed Fault	$i_{S\alpha}$, $i_{S\beta}$, ω_{est}

motor (1LA7106-4AA10) corresponding to the following parameters:

$$\begin{aligned} &P_{rated} = 4.0 \text{ kW}, \omega_{rated} = 1430 \text{ rpm}, \\ &U_n = 230/400 \text{ V}, I_n = 8.43/4.85 \text{ A}, \\ &R_S = 1.405\ \Omega, R_R = 1.395\ \Omega, \\ &L_S = L_R = 0.178 \text{ H}, L_m = 0.172 \text{ H} \end{aligned}$$

The motor speed is controlled according to the reference speed, as shown in Figure 4 , according to a load of 5 Nm. The setting speed is following to a ramp up from 0 to 500 rpm in 0.3 seconds; this speed is kept until 2 seconds and then increases to the new setting value at 750 rpm as a step function.

Three failures corresponding to each of the sensors used in the IMD system will be simulated at 1.5 seconds. The sensorless method will test the IMD with an integrated FTC function in the FOC control loop for fault detection capability and performance when operating under fault conditions.

Case 1:

The IMD is operated stably according to the reference speed; at 1.5 s, the feedback signal

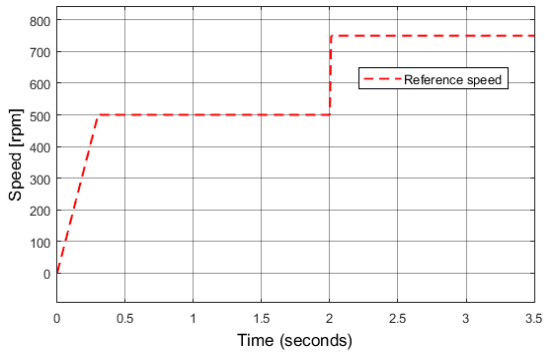

Fig. 4: Reference speed.

from the A-phase current sensor has a problem, and its value drops to 0, as shown in Figure 5(a). The FTC unit activates sensor fault diagnosis function Eq. (10); as a result, the failure of the A-phase current sensor is identified correctly, and the sensor fault flag "FA" is displayed as a high level, Figure 5(b). The FTC immediately isolates the fault current and switches the drive to current sensorless mode, corresponding to the current outputs of the FTC unit provided to the FOC controller as the estimated currents, Figure 5(c). As a result, the motor remains stable operation even under current fault conditions, as shown in Figure 5(d).

Case 2:

In the above similar case, the IMD runs according to the reference speed; B-phase current sensor fails at 1.5 s, Figure 6(a). Current sensor failure in phase B is accurately diagnosed immediately through "FB" flag, shown in Figure 6(b). The estimated stator current is used as the output of the FTC unit to supply to the FOC controller, Figure 6(c). Figure 6(d) proves the IMD can work stably under the feedback current fault.

Case 2:

In this case, the speed sensor fault is simulated at 1.5 s. The feedback speed becomes zero when a total failure occurs, as shown in Figure 7(a). The speed fault flag "Fw" increases to a high level; meanwhile, the fault indication flags of the two current sensors remain low, Figure 7(b). The output currents of the FTC unit in Figure 7(c) are the measured current and output speed is the estimated speed corresponding to Table 3. The result simulation depicted IMD's stable and sustainable operation under the speed sensor fault.

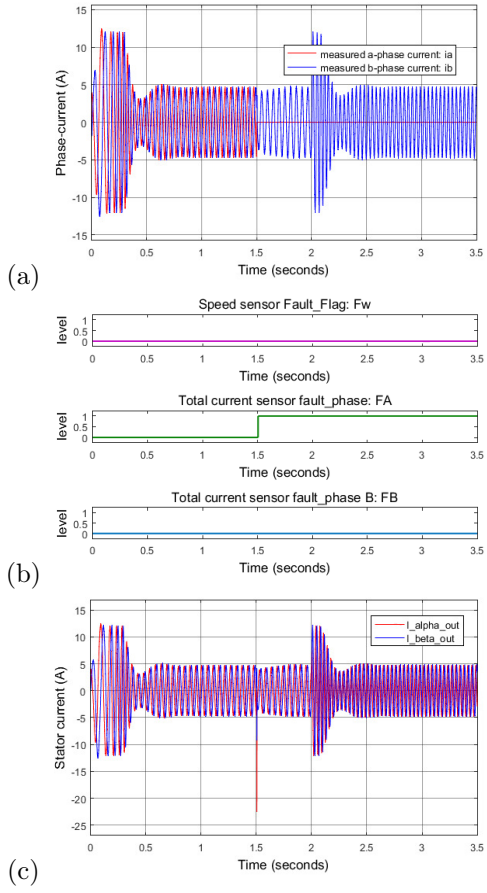

Fig. 5: (a) The fault of the A-phase stator current. (b) Sensor fault indication flags. (c) The output current of the FDI unit.

4. Conclusions

This paper presents an FTC solution for the IMD system controlling motor speed. The FTC solution consists of two main processes: fault diagnosis and reconfiguration control. The paper proposes an improved diagnosis solution based on the comparison algorithm of measured and estimated phase current for both current and speed sensor failures. The advantages of the proposed diagnosis method are fast diagnosis time,

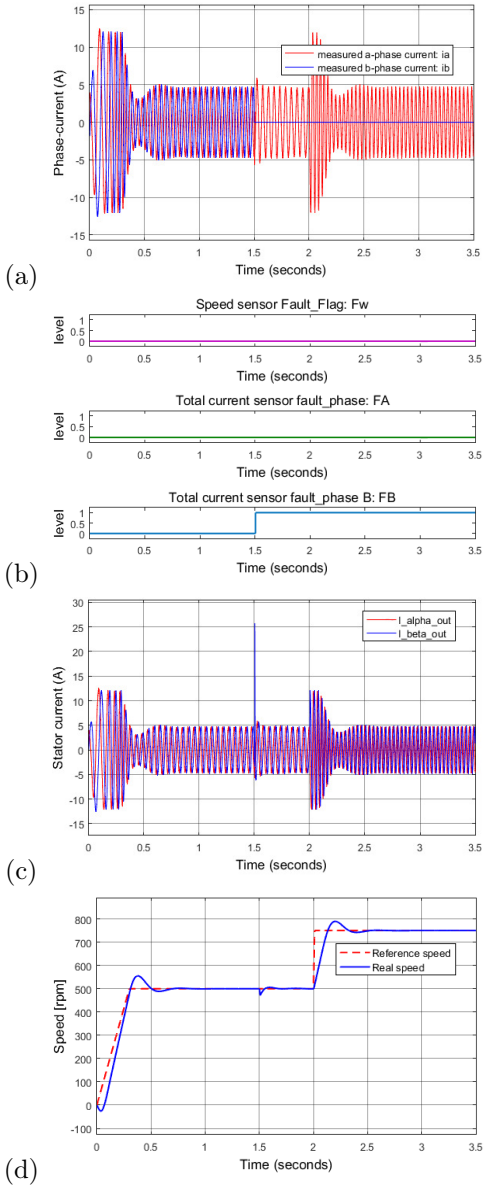

Fig. 6: (a) The fault of the B-phase stator current. (b) Sensor fault indication flags. (c) The output current of the FDI unit. (d) Speed control performance of IMD.

high accuracy, and no confusion between sensor faults. The total failure of the three sensors, including two current sensors and a speed sensor, was investigated in turn, and the results obtained were positive; the IMD system still operates stably even if the sensor fault occurs.

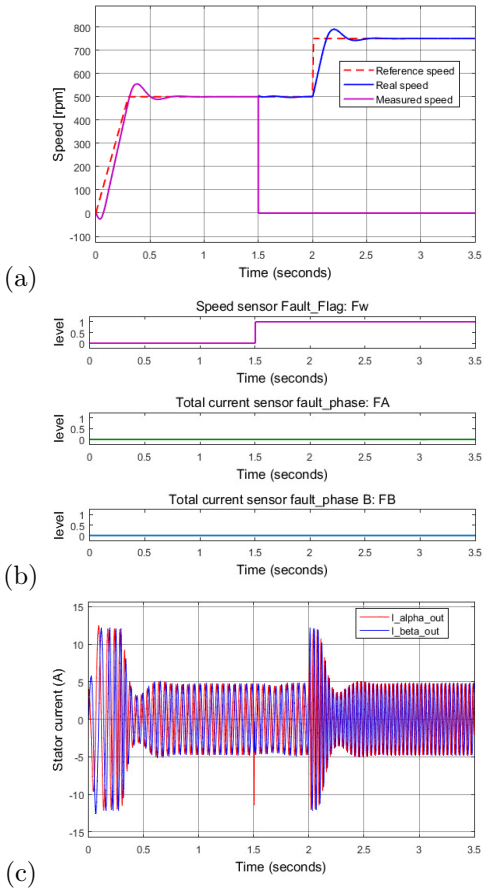

Fig. 7: (a) The fault of the speed sensor. (b) Sensor fault indication flags. (c) The output current of the FDI unit.

Acknowledgement

This research is funded by Ton Duc Thang University, Vietnam, 2022-2023, under grant number FOSTECT.2022.05.

References

[1] Ma, W. & Bai, L. (2008). Energy-saving Principles and Technologies for Induction Motors [1st Edition]. *Retrieved from http://wwwamazoncom.*

[2] Saad, N., Irfan, M., & Ibrahim, R. (2019). Condition Monitoring and Faults Diagnosis of Induction Motors: Electrical Signa-

ture Analysis [1st Edition]. *Retrieved from http://wwwamazoncom*.

[3] Faiz, J., Ghorbanian, V., & Joksimovic, G. (2017). Fault Diagnosis of Induction Motors [1st Edition]. *Retrieved from http://wwwamazoncom*.

[4] Gouichiche, A., Safa, A., Chibani, A., & Tadjine, M. (2020). Global fault-tolerant control approach for vector control of an induction motor. *International Transactions on Electrical Energy Systems*, *30*, 1–17.

[5] Jiang, J. & Yu, X. (2012). Fault-tolerant control systems: A comparative study between active and passive approaches. *Annual Reviews in Control*, *36*, 60–72.

[6] Abbaspour, A., Mokhtari, S., Sargolzaei, A., & Yen, K. (2020). A Survey on Active Fault-Tolerant Control Systems. *Electronics*, *9*, 1513.

[7] Zhao, B.Q., Z., L., Y, W., Quan, L., Hao, Y., & Ding, L. (2020). A Hybrid-Driven Elevator System With Energy Regeneration and Safety Enhancement. *IEEE Transactions on Industrial Electronics*, *67*, 7715–7726.

[8] Jo, G. & Choi, J. (2019). Gopinath Model-Based Voltage Model Flux Observer Design for Field-Oriented Control of Induction Motor. *IEEE Transactions on Power Electronics*, *34*, 4581–4592.

[9] Tran, C., Brandstetter, P., Dinh, B.H., & Dong, C.S.T. (2021). An Improving Hysteresis Current Control Method Based on FOC Technique for Induction Motor Drive. *Journal of Advanced Engineering and Computation*, *52*, 83–92.

[10] Domınguez, J., Duenas, I., & Ortega-Cisneros, S. (2020). Discrete-Time Modeling and Control Based on Field Orientation for Induction Motors. *IEEE Transactions on Power Electronics*, *35*, 8779–8793.

[11] Raisemche, A., Boukhnifer, M., Larouci, C., & Diallo, D. (2014). Two Active Fault-Tolerant Control Schemes of Induction-Motor Drive in E.V. or HEV. *IEEE Transactions on Vehicular Technology*, *63*, 19–29.

[12] Kuchar, M., Palacky, P., Simonik, P., & Strossa, J. (2021). Self-Tuning Observer for Sensor Fault-Tolerant Control of Induction Motor Drive. *Energies*, *14*, 2564.

[13] Bouakoura, M., Naït-Saïd, N., & Naït-Saïd, M. (2017). Speed Sensor Faults Diagnosis In An Induction Motor Vector Controlled Drive. *Acta Electrotechnica et Informatica*, *17*, 49–57.

[14] Azzoug, Y., Menacer, A., Pusca, R., Romary, R., Ameid, T., & Ammar, A. (2018). Fault Tolerant Control for Speed Sensor Failure in Induction Motor Drive based on Direct Torque Control and Adaptive Stator Flux Observer. *International Conference on Applied and Theoretical Electricity (ICATE), Craiova, Romania*, 1–6.

[15] Tabbache, B., Benbouzid, M., Kheloui, A., & Bourgeot, J. (2013). Virtual Sensor Based Maximum Likelihood Voting Approach for Fault-Tolerant Control of Electric Vehicle Powertrains. *IEEE Transactions on Vehicular Technology*, *62*, 1075–1083.

[16] Tran, C., Brandštetter, P., Nguyen, M., Ho, S., Dinh, B., & Pham, P. (2020). A robust diagnosis method for speed sensor fault based on stator currents in the RFOC induction motor drive. *International Journal of Electrical and Computer Engineering (IJECE)*, *10*, 3035–3046.

[17] Yu, Y., Zhao, Y., Wang, B., Huang, X., & Xu, D. (2018). Current Sensor Fault Diagnosis and Tolerant Control for VSI-Based Induction Motor Drives. *IEEE Transactions on Power Electronics*, *33*, 4238–4248.

[18] Tran, C., Brandstetterl, P., Kuchar, M., & Ho, S. (2020). A Novel Speed and Current Sensor Fault-Tolerant Control Based on Estimated Stator Currents in Induction Motor Drives. *International Review of Electrical Engineering (IREE)*, *15*, 344–351.

[19] Azzoug, Y., Sahraoui, M., Pusca, R., Tarek, A., Raphaël, R., & J.M.C, A. (2021). Current sensors fault detection and tolerant control strategy for three-phase induction

motor drives. *Electrical Engineering*, *103*, 881–898.

[20] Najafabadi, T., Salmasi, F., & Jabehdar-Maralani, P. (2011). Detection and Isolation of Speed, DC-Link Voltage and Current-Sensor Faults Based on an Adaptive Observer in Induction Motor Drives. *IEEE Transactions on Industrial Electronics*, *58*, 1662–1672.

[21] Salmasi, F. (2017). A Self-Healing Induction Motor Drive With Model Free Sensor Tampering and Sensor Fault Detection, Isolation, and Compensation. *IEEE Transactions on Industrial Electronics*, *64*, 6105–6115.

[22] Chakraborty, C. & Verma, V. (2015). Speed Current Sensor Fault Detection and Isolation Technique for Induction Motor Drive Using Axes Transformation. *IEEE Transactions on Industrial Electronics*, *62*, 1943–1954.

[23] Tran, C., Palacky, P., Sobek, M., Kuchar, M., Brandštetter, P., & Dinh, B. (2021). Current and Speed Sensor Fault Diagnosis Method Applied to Induction Motor Drive. *IEEE Access*, *9*, 38660–38672.

[24] Manohar, M. & Das, S. (2017). Current Sensor Fault-Tolerant Control for Direct Torque Control of Induction Motor Drive Using Flux-Linkage Observer. *IEEE Transactions on Industrial Informatics*, *13*, 2824–2833.

[25] Gholipour, A., Ghanbari, M., Alibeiki, E., & Mohammad, J. (2021). Speed sensorless fault-tolerant control of induction motor drives against current sensor fault. *Electrical Engineering*, *103*, 1493–1513.

[26] Tran, C., Kuchar, M., Sobek, M., Sotola, V., & Dinh, B. (2022). Sensor Fault Diagnosis Method Based on Rotor Slip Applied to Induction Motor Drive. *Sensors*, *22*, 8636.

[27] Adamczyk, M. & Orlowska-Kowalska, T. (2019). Virtual current sensor in the fault-tolerant field-oriented control structure of an induction motor drive. *Sensors*, *19*, 4979.

[28] Brandštetter, P. (2012). Sensorless control of induction motor using modified MRAS. *International Review of Electrical Engineering*, *7*, 4404–4411.

[29] Zbede, Y., Gadoue, S., & Atkinson, D. (2016). Model predictive MRAS estimator for sensorless induction motor drives. *IEEE Transactions on Industrial Electronics*, *63*, 3511–3521.

[30] Azzoug, Y., Sahraoui, M., Pusca, R., Ameid, T., Romary, R., & Cardoso, A. High-performance vector control without AC phase current sensors for induction motor drives: Simulation and real-time implementation. *ISA transactions*, *109*, 295–306.

About Authors

Cuong Dinh TRAN was born in Vietnam. He received his Ph.D. in Electrical Engineering from VSB-Technical University of Ostrava, Czech Republic, in 2020. Now, he is a lecturer at the Faculty of Electrical-Electronic Engineering at Ton Duc Thang University, Ho Chi Minh City, Vietnam. His research interests are the application of modern control methods and intelligent algorithms in induction motor drives.

Giang Thi Tuyet LAI was born in Vietnam in 2002. Now, she is a student at the Faculty of Electrical-Electronic Engineering at Ton Duc Thang University, Ho Chi Minh City, Vietnam. Her research interests are the application of modern control methods and intelligent algorithms in induction motor drives. She is a member of the student research group on "modern control methods of AC machines."

Thao Minh CA was born in Vietnam in 2001. Now, he is a student at the Faculty of Electrical-Electronic Engineering at Ton Duc Thang University, Ho Chi Minh City, Vietnam. His research interests are the application of modern control methods and intelligent algorithms in induction motor drives. He is a member of the student research group on "modern control methods of AC machines".

Thong Tien NGUYEN was born in Vietnam in 1998. He received a Bachelor's degree in Electrical Engineering from Ton Duc Thang University, Ho Chi Minh City, Vietnam in 2021. He is currently a freelancer and a researcher in Electrical Motor Field. His research is mainly about control methods and machine learning algorithms in induction motor drives.

Phuong Duy NGUYEN was born in Vietnam. He received B.E degree from Ho Chi Minh City University of Technology and Education and M.E degree from Ho Chi Minh City University Of Technology, Vietnam, in 2010 and 2014. Now, he is a lecturer in the Electrical Engineering Department, Faculty of Electronics and Telecommunications at Saigon University, Ho Chi Minh City, Vietnam. His research interests are the application of modern control methods and intelligent algorithms in induction motor drives. He is a member of the research group on "modern control methods of AC machines."